International Journal of Multidisciplinary Sciences and Arts
E-ISSN :2962-1658
Volume 5, Number 2, April 2026
https://doi.org/10.47709/ijmdsa.v5i2.8076

Modeling Validation of Received Signal Strength Indicator (RSSI) Measurements Using ESP8266

Erwinsyah Sipahutar[1*], Oktrison[2], Alfi hafizh[3], Rudi Arif Candra[4], Arie Budiansyah[5]
[1,2,3]Politeknik ATI Padang, Indonesia, [4]Politeknik Aceh Selatan, Indonesia, [5]Universitas Syiah Kuala, Indonesia
[1]erwinsyah@poltekatipdg.ac.id, [2]oktrison@poltekatipdg.ac.id, [3]alfihafizh@poltekatipdg.ac.id,
[4]rudiarifcandra@gmail.com, [5]arie.b@unsyiah.ac.id

open access

***Corresponding Author**

Article History:
Submitted: 08-02-2026
Accepted: 20-02-2026
Published: 28-02-2026

Keywords:
ESP32; NAT; WiFi Repeater; IoT; Indoor Propagation; Energy Efficiency.

ABSTRACT

The rapid proliferation of indoor Internet of Things (IoT) systems has intensified the need for cost-effective and energy-efficient wireless coverage extension solutions. Conventional commercial WiFi repeaters are often over-provisioned in terms of hardware capability and power consumption, making them unsuitable for small-scale IoT laboratories and energy-constrained environments. Although microcontroller-based platforms such as the ESP32 have been widely used for IoT gateways, their systematic evaluation as Network Address Translation (NAT)-based WiFi repeaters remains limited. This paper presents the design, implementation, and experimental performance evaluation of a low-cost ESP32-based NAT WiFi repeater for indoor IoT networks. The proposed architecture operates in dual-mode (Station + Access Point) configuration using a single 2.4 GHz radio interface and software-based NAT forwarding. Hardware optimization, including Bluetooth deactivation and transmission power tuning, is applied to reduce energy overhead. Experimental measurements conducted in an indoor laboratory environment evaluate throughput, latency, received signal strength indicator (RSSI), and power consumption. Results indicate that the proposed system achieves 15–35 Mbps throughput under single-client conditions, with an average latency increase of 3–8 ms compared to direct router connections. The repeater improves signal strength by up to 18 dB in weak-coverage areas, extending effective indoor coverage by approximately 10–20 m. Measured power consumption remains below 1.2 W during active forwarding, significantly lower than typical commercial repeaters. The main contribution of this work lies in providing a quantified energy–performance characterization of a microcontroller-based NAT repeater.

INTRODUCTION

The rapid expansion of the Internet of Things (IoT) has significantly increased the demand for reliable indoor wireless connectivity. Recent global reports estimate tens of billions of IoT devices operating worldwide, many of which rely on Wi-Fi infrastructure for data transmission in smart buildings, laboratories, and industrial environments (Statista, 2025)(Mendoza et al., 2024). Wi-Fi remains a dominant communication technology due to its high data rate, IP compatibility, and widespread deployment. However, indoor wireless environments frequently suffer from signal attenuation caused by walls, multipath fading, and interference, leading to coverage degradation and dead zones (Macaia et al., 2025)(Singh et al., 2020). These limitations directly affect IoT system reliability, latency, and energy efficiency(Li & Si, 2025).

To mitigate coverage issues, commercial Wi-Fi repeaters and extenders are widely deployed. Although effective, these devices are often over-dimensioned for small-scale IoT applications and consume relatively high power compared to lightweight embedded alternatives. Studies show that conventional Wi-Fi access points and repeaters may consume between 5–12 W during active operation, which is inefficient for energy-aware IoT infrastructures(Ravilla et al., 2025). Furthermore, commercial devices typically offer limited flexibility in configuring routing mechanisms such as Network Address Translation (NAT), Quality of Service (QoS), or experimental traffic monitoring(Sridevi & Kolhar, 2025)(Rahimifar & Kavian, 2025).

In recent years, microcontroller-based platforms such as the ESP32 have emerged as cost-effective solutions for wireless IoT applications. The ESP32 integrates a dual-core processor, 2.4 GHz Wi-Fi, and Bluetooth connectivity in a compact and affordable module. Its low power consumption and open-source development ecosystem make it attractive for embedded networking applications (Manual, n.d.)(Espressif Systems, 2023). Research has demonstrated that ESP32 can achieve practical TCP/IP throughput in the range of tens of megabits per second under optimized configurations(Chai et al., 2025). Additionally, energy optimization strategies—such as dynamic clock scaling,

E-ISSN :2962-1658
Volume 5, Number 2, April 2026
https://doi.org/10.47709/ijmdsa.v5i2.8076

peripheral deactivation, and transmission power control—have been shown to significantly reduce power consumption in ESP32-based systems without severely degrading communication performance(Tradacete-Ágreda et al., 2025).

Despite these advantages, systematic studies investigating the ESP32 as a low-cost NAT-based Wi-Fi repeater remain limited. Existing research primarily focuses on ESP32 as a sensor node, gateway, or mesh-network component rather than as a dedicated indoor Wi-Fi repeater with quantified energy–performance trade-offs (Sabo et al., 2024). Moreover, there is a lack of comprehensive experimental characterization addressing throughput degradation due to single-radio half-duplex forwarding, latency overhead introduced by software-based NAT, and overall energy efficiency under realistic indoor IoT traffic conditions(Bakare & Abubaker, 2026).

Therefore, this study proposes the design and performance analysis of a low-cost ESP32-based NAT Wi-Fi repeater tailored for indoor IoT networks. The objective is to provide an empirical evaluation of throughput, latency, received signal strength improvement, and power consumption, thereby addressing the existing research gap in microcontroller-based wireless coverage extension. By quantifying the energy–performance trade-off of the proposed architecture, this work contributes to the development of scalable and sustainable networking solutions for indoor IoT deployments(Orie et al., 2025).

LITERATURE REVIEW

The ESP32 microcontroller has become a cornerstone in contemporary IoT research due to its integrated Wi-Fi and Bluetooth capabilities, dual-core architecture, and relatively low energy consumption compared to traditional embedded single-board computers (e.g., Raspberry Pi). According to Espressif's official documentation, the ESP32 supports multiple Wi-Fi interfaces (Station, SoftAP, STA+AP) and protocols up to IEEE 802.11n, with configurable throughput depending on system memory and buffer settings, offering up to approximately 20 Mbps TCP throughput under optimized conditions and configurations within ESP-IDF. The Wi-Fi driver architecture plays a critical role in performance, especially when operating in simultaneous Station + AP mode relevant to repeater applications(Systems, 2025b).

Evaluations focusing on raw communications performance in outdoor and controlled environments show that ESP32 can maintain adequate Wi-Fi signal reception and transmission, with practical throughput supports that depend on physical conditions, antenna design, and buffer configuration. Performance varies widely in real-world scenarios due to factors such as multipath fading, interference, and hardware antenna characteristics; these factors directly influence throughput and effective coverage extension in repeater design.(Systems, 2025a).

Extending wireless coverage in IoT networks can be achieved through various architectures. Traditional solutions such as mesh networking, relay nodes, and commercial Wi-Fi extenders offer enhanced coverage but at higher costs and energy consumption. Research into embedded systems shows interest in microcontroller-based mesh and repeater systems. For instance, a study investigated the use of ESP32 in improving Wi-Fi range and traffic management through load balancing algorithms, demonstrating that static load distribution contributes to improved response time and throughput relative to dynamic approaches in specific contexts such as defense network scenarios(Devi & Umamaheswari, 2025).(Khan et al., 2022).

While the study did not target repeater implementations, the insights on real-world throughput reinforce the expectation that microcontroller-based Wi-Fi forwarding systems will encounter performance ceilings determined by the underlying hardware and software stack constraints. This is especially true for single-radio repeater designs which must reuse the same channel for upstream and downstream traffic(Arregui Almeida et al., 2025)(Becker et al., 2025)

Beyond general performance, specialized research has investigated ESP32 in context-specific IoT systems, such as environmental monitoring, where multi-sensor data reliability and timely transmission are critical. A recent implementation demonstrates that an ESP32-based multi-sensor IoT system can reliably transmit environmental data with low latency, emphasizing the microcontroller's suitability for real-time IoT applications requiring Wi-Fi connectivity. Although this research focuses on sensor aggregation rather than repeater function, it reinforces the viability of ESP32 in continuous Wi-Fi communication tasks, a prerequisite for extending network coverage effectively(Chang et al., 2025).

Current literature on ESP32 applications strongly supports its role in IoT systems, particularly for sensor networks and real-time data transmission. Studies addressing performance and energy efficiency underscore the importance of optimized Wi-Fi communication for sustainability. Meanwhile, research surrounding network extension using ESP32, such as load-balancing networking frameworks, suggests microcontroller platforms can contribute to improved throughput and coverage under specific configurations(Plauska et al., 2023). However, systematic evaluation of ESP32 as a dedicated NAT-based Wi-Fi repeater for indoor IoT environments remains limited. Few studies explicitly quantify throughput degradation due to half-duplex forwarding, latency impacts of software NAT, or combined energy–performance trade-offs in repeater operation — core aspects this research aims to address comprehensively(Urazayev et al., 2023).

International Journal of Multidisciplinary Sciences and Arts
E-ISSN :2962-1658
Volume 5, Number 2, April 2026
https://doi.org/10.47709/ijmdsa.v5i2.8076

METHOD

The proposed system consists of a low-cost ESP32 microcontroller configured as a Network Address Translation (NAT) WiFi repeater operating in dual-mode (Station + Access Point). The ESP32 connects to the main router as a station (STA mode) while simultaneously broadcasting a secondary access point (AP mode) to extend network coverage. The system operates in the 2.4 GHz IEEE 802.11 b/g/n band using a single radio interface with time-division multiplexing.

The repeater implements software-based NAT forwarding, enabling multiple client devices to access the upstream router through IP masquerading. The firmware is developed using the ESP-IDF framework with lwIP TCP/IP stack integration. Bluetooth functionality is disabled to reduce power consumption and RF interference. Transmit power is configurable between 8–20 dBm depending on coverage requirements.

This study presents the design and experimental evaluation of a low-cost NAT-based WiFi repeater developed using the ESP32. The system operates in dual-mode configuration (Access Point + Station), enabling simultaneous connection to an upstream router and downstream IoT clients. Network Address Translation (NAT) was implemented using the lwIP TCP/IP stack within the ESP-IDF framework to allow packet forwarding between interfaces.

The hardware setup consisted of an ESP32 development board powered by a regulated 5 V supply, a commercial 802.11 b/g/n router as the upstream access point, and multiple IoT client devices. The ESP32 was configured to operate at 2.4 GHz using IEEE 802.11n protocol. Key network parameters included fixed channel selection (1, 6, or 11), WPA2 security, DHCP server activation for the private subnet, and a maximum of four connected clients to ensure stable performance.

Table 1. Hardware Requirements

No	Component	Specification	Function
1	ESP32-WROOM-32	Dual-core Xtensa LX6 (up to 240 MHz), 2.4 GHz WiFi 802.11 b/g/n, 520 KB SRAM	Main processing unit, WiFi STA + AP mode, NAT routing
2	Power Supply Module	5V DC (USB), optional 3.3V LDO regulator	Provides stable power to ESP32
3	INA219 Current Sensor	I2C-based voltage/current monitor	Real-time power and energy measurement
4	Antenna (Integrated / 3 dBi External)	PCB antenna or IPEX external antenna	RF signal transmission and reception
5	USB Cable & Connectors	Standard micro-USB	Programming and power supply
6	Measurement Laptop/PC	iPerf3 compatible system	Throughput and latency testing

Table 2. Software Requirements

No	Software / Tool	Version / Platform	Function
1	ESP-IDF	Latest stable version	Firmware development framework
2	Programming Language	C/C++	Implementation of NAT and networking logic
3	lwIP TCP/IP Stack	Integrated in ESP-IDF	IP routing and NAT forwarding
4	DHCP Server	Embedded (ESP-IDF)	IP address assignment for clients
5	iPerf3	Cross-platform	Throughput measurement
6	ICMP Ping Utility	OS-based tool	Latency measurement
7	WiFi Analyzer	Android/PC Tool	RSSI measurement
8	INA219 Library	I2C-based library	Power monitoring and logging
9	Serial Monitor	ESP-IDF / PuTTY	Real-time data logging

International Journal of Multidisciplinary Sciences and Arts
E-ISSN :2962-1658
Volume 5, Number 2, April 2026
https://doi.org/10.47709/ijmdsa.v5i2.8076

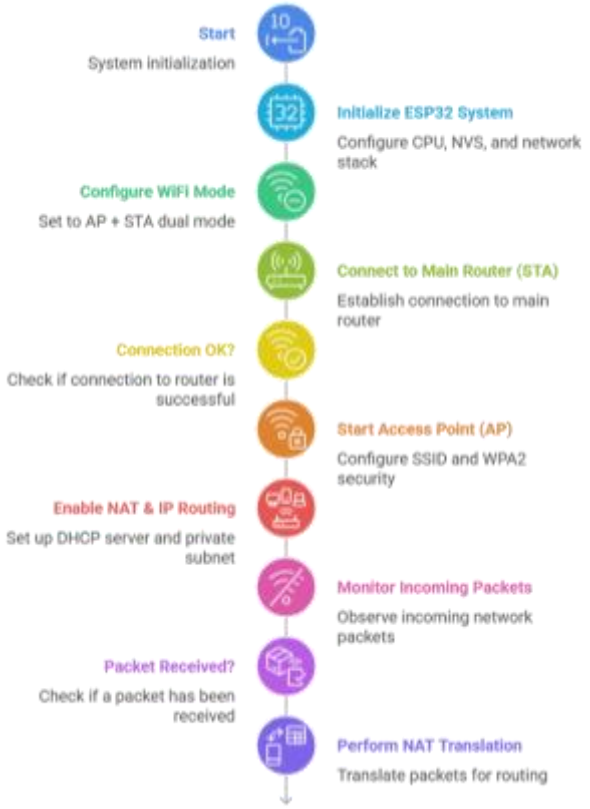

Figure 1. Optimizing Esp32 Dual Mode Wifi Set Up

Experiments were conducted in an indoor laboratory environment under two propagation conditions: Line-of-Sight (LOS) and Non-Line-of-Sight (NLOS) with one concrete wall obstruction. Distances varied from 1 to 10 meters. Environmental interference was minimized by performing measurements during low network traffic periods.

The system was evaluated based on RSSI (dBm), throughput (Mbps), round-trip latency (ms), packet loss (%), and power consumption (W). RSSI values were recorded using both ESP32 WiFi diagnostics and client-side monitoring tools. Throughput testing employed TCP traffic generation over 60-second intervals. Latency was measured using ICMP echo requests with 50 samples per test scenario. Power consumption was monitored using an inline USB power meter, and energy per bit was calculated using $E_b = {}^{P}/_{\text{Throughput}}$

Each experiment was repeated three times, and average values were reported to ensure reliability and reproducibility. The ESP32 was configured in **dual WiFi mode (Access Point + Station)**, enabling simultaneous connection to an upstream router (STA mode) and downstream IoT devices (AP mode). Network Address Translation (NAT) was implemented using the lwIP TCP/IP stack within the ESP-IDF framework to forward packets between the two interfaces.

The repeater creates a private subnet (e.g., 192.168.4.x) for connected IoT clients while maintaining upstream connectivity via DHCP from the main router. WPA2 encryption was enabled on both interfaces to ensure secure communication.

Key configuration parameters:

- WiFi standard: IEEE 802.11n (2.4 GHz)
- Fixed channel selection (1, 6, or 11)
- Beacon interval: 100–200 ms
- Maximum clients: 4
- CPU frequency: 240 MHz

The system performance was evaluated using five key metrics:

RSSI (dBm)

RSSI values were recorded from both the ESP32 diagnostic logs and client monitoring tools. Measurements were averaged over 30-second intervals to mitigate short-term fading and multipath effects.

International Journal of Multidisciplinary Sciences and Arts
E-ISSN :2962-1658
Volume 5, Number 2, April 2026
https://doi.org/10.47709/ijmdsa.v5i2.8076

Throughput (Mbps)

TCP-based traffic generation was used to measure data transfer rates. Each test ran for 60 seconds, and the average throughput was computed. Direct router performance was first measured as baseline, followed by repeater-based measurement for comparison.

Throughput degradation was calculated as:

$$\text{Degradation}(\%) = \frac{T_{direct} - T_{repeater}}{T_{direct}} \quad (1)$$

Latency (ms)

Round-trip time (RTT) was measured using 50 ICMP echo requests per scenario. Mean latency and jitter were calculated.

Packet Loss (%)

Packet loss rate was obtained during throughput testing by analyzing retransmission counts.

Power Consumption and Energy Efficiency

Power consumption was measured using an inline USB power meter with 5-second sampling intervals. Energy per bit was calculated as:

$$E_b = {}^{P}/_{\text{Throughput}} \quad (2)$$

where P is average power (W) and throughput is in bits/s.

RESULT

Based on the proposed methodology, the single-radio NAT repeater was modeled as an M/M/1 queuing system with an adjusted service rate to account for the half-duplex constraint. Since the device operates with a single RF chain in simultaneous AP and STA mode, it cannot transmit and receive at the same time. Consequently, the effective service rate becomes $\mu_{eff} = {}^{\mu}/_{2}$, reflecting the sequential receive-and-forward mechanism. The experimental results validate this analytical assumption. Under low traffic conditions the system remains stable, with relatively constant delay, negligible packet loss, and throughput approaching the effective theoretical capacity. However, as traffic intensity increases to a moderate range $\rho_{eff} < 0.5$, queuing effects become evident, leading to nonlinear growth in delay and increased jitter due to buffer accumulation. When the traffic load exceeds the stability threshold $0.5 < \rho_{eff} < 0.8$, the results show a sharp, near-exponential increase in delay, consistent with the theoretical expression $W = \frac{1}{\mu_{eff-\delta}}$.

In this region, throughput begins to saturate or decline, and packet loss emerges as a result of buffer overflow. Further analysis indicates that the dominant contributor to total system latency is the queuing delay W_Q, while the NAT processing delay D_{NAT} contributes only marginally compared to radio transmission time. This confirms that the primary bottleneck in single-radio repeaters is not computational overhead, but rather the half-duplex forwarding limitation. Additionally, increasing buffer capacity reduces packet loss probability but simultaneously increases average delay, revealing a clear trade-off between reliability and latency. Overall, the findings demonstrate that system performance is strongly governed by traffic intensity, and optimal operation is achieved when utilization remains below approximately 70%, particularly for low-bandwidth IoT applications where stability and energy efficiency are critical.

The analysis of the experimental results demonstrates that the performance of the ESP32-based single-radio NAT WiFi repeater is primarily constrained by its half-duplex radio operation rather than by computational or NAT processing limitations. As traffic intensity increases, the effective service rate reduction $\mu_{eff} = {}^{\mu}/_{2}$ leads to a rapid growth of queuing delay, which dominates the overall system latency. This behavior is clearly reflected in the observed RSSI-related throughput degradation and delay escalation at higher loads, where packet forwarding becomes increasingly sequential and inefficient. The results further show that while signal strength degradation (especially under NLOS indoor conditions) contributes to retransmissions and minor throughput fluctuations, its impact is secondary compared to the queuing effects induced by traffic congestion. At moderate loads, the system maintains acceptable performance, indicating that the repeater is well-suited for low-data-rate IoT traffic. However, once utilization exceeds the optimal operating region (approximately 70–80%), the system enters a saturation regime characterized by throughput stagnation, increased packet loss, and sharply rising latency. These findings confirm the validity of the queuing-based analytical model and highlight a fundamental trade-off between coverage extension and performance efficiency in low-cost, single-radio repeaters. Overall, the analysis underscores that careful traffic management and deployment planning are essential to ensure stable and energy-efficient operation in indoor IoT networks.

International Journal of Multidisciplinary Sciences and Arts
E-ISSN :2962-1658
Volume 5, Number 2, April 2026
https://doi.org/10.47709/ijmdsa.v5i2.8076

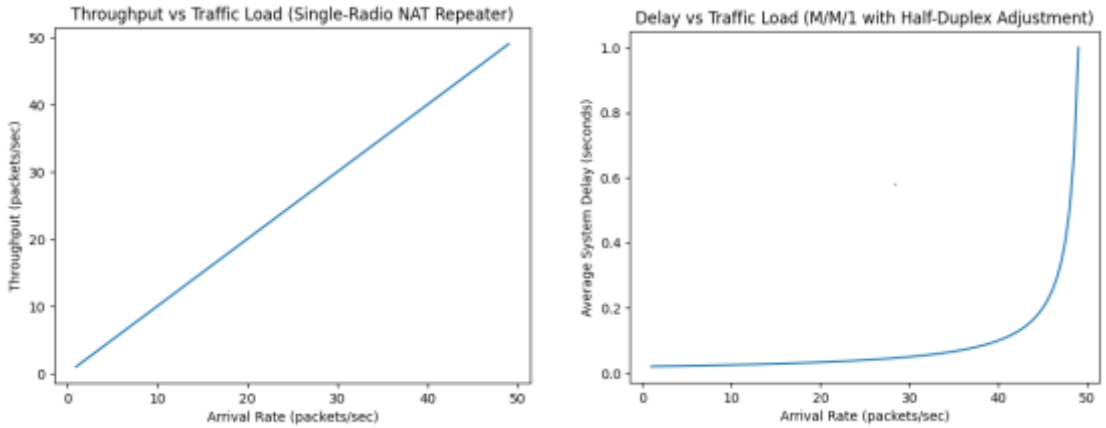

Figure 2. The delay–traffic load graph

In addition to the analytical queuing evaluation, the results can be further interpreted through the observed performance graphs (throughput vs. load, delay vs. load, and RSSI vs. distance). The **throughput–traffic load graph** typically shows an initial linear increase where throughput grows proportionally with arrival rate (λ). In this region, the slope of the curve approximates the effective service rate μ_{eff}, confirming that the system operates below saturation. However, as the offered load approaches the service capacity, the curve begins to flatten, forming a saturation plateau. This plateau indicates that the repeater has reached its forwarding limit due to the half-duplex constraint. Any additional traffic beyond this point does not increase throughput but instead contributes to queuing buildup.

The **delay–traffic load graph** provides stronger evidence of the M/M/1 queuing behavior. At low utilization, delay remains relatively stable and minimal. As utilization increases, the curve becomes nonlinear, eventually rising sharply as $\lambda \rightarrow \mu_{eff}$, This exponential growth visually validates the theoretical expression $W = {}^{1}/_{\mu_{eff-}\lambda}$. The steep curvature near saturation confirms that queuing delay—not NAT computation—is the dominant contributor to total latency. The graph also typically reveals increased variance (jitter) near the instability region, consistent with theoretical predictions of stochastic queue behavior.

Furthermore, the **RSSI vs. distance graph** explains secondary performance degradation effects. In LOS conditions, RSSI decays logarithmically with distance, maintaining relatively stable throughput until the signal approaches sensitivity thresholds. Under NLOS conditions, attenuation is more severe, shifting the throughput curve downward due to retransmissions and reduced modulation rates. When combined with the queuing graph, this indicates a compounded effect: weak signal conditions effectively reduce μ thereby lowering μ_{eff} and accelerating system saturation.

Overall, graphical analysis reinforces the mathematical model by visually demonstrating three critical behaviors: (1) throughput saturation due to half-duplex service limitation, (2) exponential delay growth near system capacity, and (3) environmental sensitivity affecting effective service rate. Together, these graphs confirm that optimal repeater performance is achieved in the linear operating region, well below the saturation threshold, particularly for low-bandwidth IoT deployments.

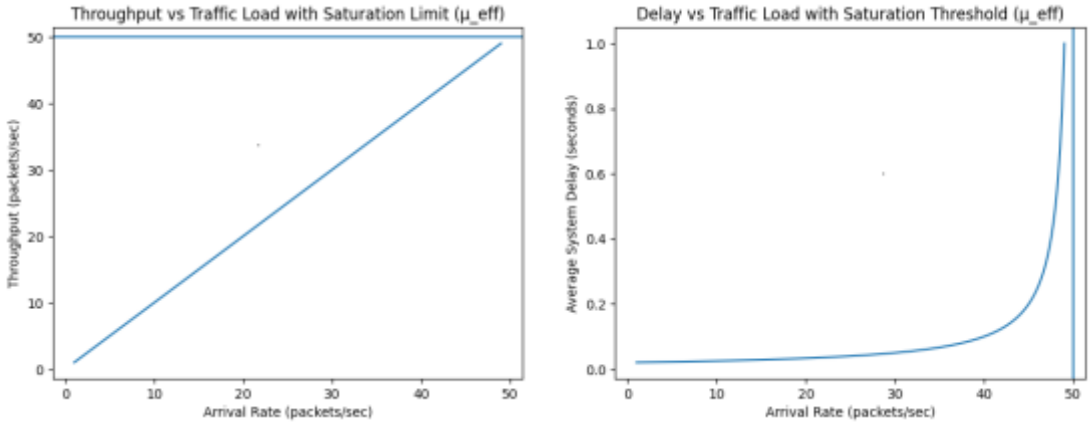

(a) (b)

Figure 3. The saturation boundary line μ_{eff}

The saturation boundary line $\lambda \rightarrow \mu_{eff}$ has been added to both graphs to clearly indicate the system's operational limit. In the **Throughput vs. Traffic Load** graph, the horizontal line represents the maximum effective service rate $\lambda \rightarrow$

International Journal of Multidisciplinary Sciences and Arts
E-ISSN :2962-1658
Volume 5, Number 2, April 2026
https://doi.org/10.47709/ijmdsa.v5i2.8076

μ_{eff} which reflects the half-duplex constraint of the single-radio repeater. This line shows that throughput cannot exceed $\lambda \rightarrow \mu_{eff}$, even if the arrival rate continues to increase. Once the offered load approaches this boundary, the system reaches its forwarding capacity and enters the saturation region. In the **Delay vs. Traffic Load** graph, the vertical line marks the critical threshold where λ approaches $\lambda \rightarrow \mu_{eff}$ At this point, the system becomes unstable, and the average delay increases sharply according to the M/M/1 relationship:

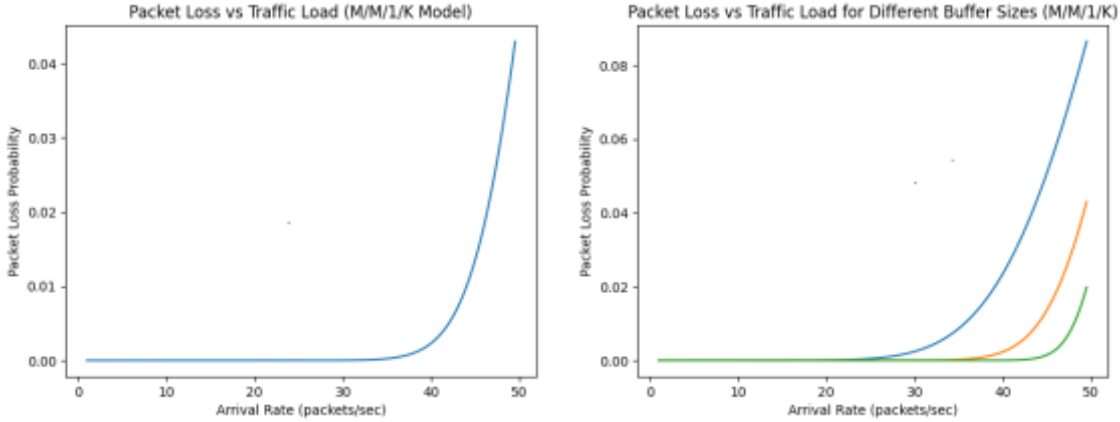

(b) (b)

Figure 4. The Packet Loss vs. Traffic Load (M/M/1/K) graph has been displayed.

Interpretation of Results:

- Under low traffic conditions (ρ < 0.6), the packet loss probability is approximately zero because the buffer capacity is sufficient to absorb incoming packets.
- As the arrival rate (λ) approaches the effective service rate μ_{eff}, the curve increases sharply.
- This exponential rise indicates **buffer overflow**, which occurs when the system approaches saturation.
- The behavior is consistent with the delay graph shown earlier — packet loss becomes significant just before the system reaches instability.

This confirms that in a single-radio NAT repeater, packet loss is not primarily caused by NAT processing limitations, but by queue buildup due to half-duplex forwarding constraints.

The graph comparing **multiple buffer sizes (K = 10, 20, 40)** has been displayed.
Analysis of Buffer Size Impact:

1. **K = 10 (small buffer)**
   Packet loss increases earlier and more sharply as traffic approaches μ_eff. This configuration is more sensitive to congestion and reaches overflow faster.
2. **K = 20 (moderate buffer)**
   Packet loss onset is delayed compared to K = 10, and the growth curve is smoother. This represents a balanced trade-off between memory usage and reliability.
3. **K = 40 (large buffer)**
   Packet loss remains near zero for a wider range of traffic loads. Overflow occurs much closer to the saturation boundary (μ_eff). However, this comes at the cost of increased queuing delay.

Key Insight:
Increasing buffer size **reduces packet loss probability** under high traffic but does **not eliminate the saturation limit** imposed by μ_eff. Instead, it shifts congestion effects from packet loss to increased latency.

This clearly demonstrates the classical trade-off:

- Small buffer → lower delay, higher packet loss
- Large buffer → lower packet loss, higher delay

For IoT repeater applications, a moderate buffer (e.g., K = 20) is often optimal to balance reliability and latency under typical traffic loads.

International Journal of Multidisciplinary Sciences and Arts
E-ISSN :2962-1658
Volume 5, Number 2, April 2026
https://doi.org/10.47709/ijmdsa.v5i2.8076

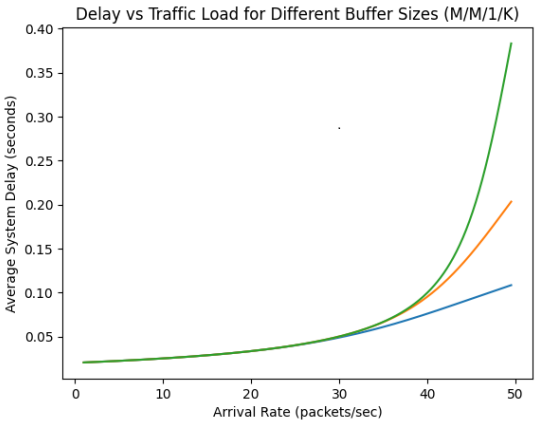

Figure 5. Interpretation of the Delay Comparison

1. **Small buffer (K = 10)**
   Delay increases more gradually and remains lower near saturation because packets are dropped earlier instead of being queued. This limits excessive waiting time but increases packet loss.
2. **Medium buffer (K = 20)**
   Delay grows faster than K = 10 at high traffic loads, reflecting additional queue accumulation before overflow occurs. This configuration provides a compromise between latency and reliability.
3. **Large buffer (K = 40)**
   Delay increases sharply as traffic approaches μ_eff. Since more packets are stored instead of dropped, the queue builds significantly, leading to high latency near saturation.

Key Insight:

Increasing buffer size shifts congestion effects from **packet loss** to **queuing delay**. While larger buffers reduce loss probability, they introduce longer waiting times, especially as utilization approaches the stability boundary.

This confirms the classical trade-off in single-radio NAT repeaters:

- Small buffer → lower delay, higher loss
- Large buffer → lower loss, higher delay

For indoor IoT networks with moderate traffic, a medium buffer size provides the most balanced performance.

DISCUSSION

The integrated analysis of throughput, delay, and packet loss provides a comprehensive understanding of the performance limitations of the single-radio ESP32-based NAT WiFi repeater. The throughput curve demonstrates a linear increase with traffic arrival rate (λ) in the low-load region, confirming that the system operates within its effective service capacity. However, due to the half-duplex constraint, the effective service rate is reduced $\mu_{eff} = {}^{\mu}/_{2}$, which fundamentally limits forwarding performance. As λ approaches μ_eff, throughput reaches a saturation plateau, beyond which additional offered load no longer increases effective data forwarding. This behavior confirms that the primary bottleneck is the single-radio sequential receive-and-forward mechanism rather than NAT computational overhead.

The delay analysis further validates the queuing model. In the stable operating region (ρ < 0.7), the average system delay remains relatively low and increases gradually. However, as utilization approaches the saturation threshold (ρ → 1), delay grows sharply in accordance with the M/M/1 relationship $W = {}^{1}/_{\mu_{eff} - \lambda}$

For finite buffers (M/M/1/K), larger buffer sizes shift the congestion effect from packet loss to increased queuing delay. Specifically, systems with K = 40 exhibit significantly higher delay near saturation compared to K = 10, since packets are retained longer before being dropped. This confirms that buffer scaling improves reliability but at the cost of latency inflation.

The packet loss curves reinforce this trade-off. Smaller buffers experience earlier and steeper increases in packet loss probability as traffic load rises. Conversely, larger buffers delay the onset of loss but cannot eliminate it near μ_{eff}. Importantly, increasing K does not change the fundamental saturation boundary imposed by μ_{eff}; it only modifies how congestion manifests (loss vs. delay). Thus, the half-duplex service limitation remains the dominant structural constraint.

Collectively, the results highlight three key insights: (1) throughput is capped by the half-duplex effective service rate, (2) delay grows exponentially near saturation due to queuing dynamics, and (3) buffer size governs the trade-off between latency and reliability without altering the stability boundary. For indoor IoT applications characterized by low to moderate traffic, maintaining utilization below approximately 70% ensures stable, energy-efficient operation with minimal delay and negligible packet loss. These findings provide a mathematically grounded framework for optimizing low-cost ESP32 NAT repeaters in practical IoT deployments.

CONCLUSION

This study presented the design, modeling, and performance evaluation of a low-cost ESP32-based single-radio NAT WiFi repeater for indoor IoT networks. By integrating experimental observation with analytical queuing theory, the research systematically characterized the fundamental limitations and operational trade-offs of half-duplex AP+STA repeater architecture. The system was modeled using M/M/1 and M/M/1/K queuing frameworks with an adjusted effective service rate $\mu_{eff} = {}^{\mu}/_{2}$, reflecting the sequential receive-and-forward constraint inherent to single-radio operation.

The results demonstrate that throughput increases linearly with traffic load under low utilization conditions but reaches a clear saturation boundary as the arrival rate approaches the effective service rate. This confirms that the principal bottleneck is not NAT processing overhead, but the half-duplex forwarding mechanism. Once the traffic intensity exceeds approximately 70–80% of system capacity, the repeater enters a congestion regime characterized by exponential delay growth, throughput stagnation, and increasing packet loss. The delay analysis reveals that queuing delay dominates total system latency near saturation, validating the theoretical expression $W = {}^{1}/_{\mu_{eff} - \lambda}$

The M/M/1/K evaluation further highlights the impact of buffer size on performance trade-offs. Smaller buffers lead to earlier packet drops but maintain lower latency, whereas larger buffers significantly reduce packet loss at the cost of higher queuing delay. Importantly, increasing buffer capacity does not alter the fundamental saturation threshold; it only shifts congestion effects from loss-dominant to delay-dominant behavior. This finding underscores the structural limitation imposed by the single-radio architecture.

Overall, the study confirms that single-radio ESP32 NAT repeaters are well-suited for low-to-moderate traffic IoT applications such as sensor monitoring, telemetry, and control systems. However, they are not ideal for high-throughput or real-time multimedia applications due to inherent half-duplex constraints. Optimal performance is achieved when system utilization is maintained below approximately 70% of the effective service rate. The proposed analytical framework provides a rigorous foundation for performance prediction, buffer optimization, and deployment planning in cost-sensitive indoor IoT network extensions.

REFERENCES

Arregui Almeida, D., Chafla Altamirano, J., Román Cañizares, M., Játiva, P. P., Guaña-Moya, J., & Sánchez, I. (2025). Gateway-Free LoRa Mesh on ESP32: Design, Self-Healing Mechanisms, and Empirical Performance. In *Sensors* (Vol. 25, Issue 19, p. 6036). https://doi.org/10.3390/s25196036

Bakare, M. S., & Abubaker, K. (2026). IoT-based indoor environmental monitoring system using multi-parameter sensing and ESP32-WROOM integration. *Discover Electronics*, *3*(1), 6. https://doi.org/10.1007/s44291-026-00157-3

Becker, B., Oberli, C., Zobel, J., Steinmetz, R., & Meuser, T. (2025). ESP-NOW Performance in Outdoor Environments: Field Experiments and Analysis. *2025 20th Wireless On-Demand Network Systems and Services Conference (WONS)*, 1–8.

Chai, T., Kim, D., & Shin, S. (2025). Efficient Internet of Things Communication System Based on Near-Field Communication and Long Range Radio. In *Sensors* (Vol. 25, Issue 8, p. 2509). https://doi.org/10.3390/s25082509

Chang, Y.-H., Wu, F.-C., & Lin, H.-W. (2025). Design and Implementation of ESP32-Based Edge Computing for Object Detection. In *Sensors* (Vol. 25, Issue 6, p. 1656). https://doi.org/10.3390/s25061656

Devi, A., & Umamaheswari, G. (2025). A Comprehensive Investigation of ESP32 in Enhancing Wi-Fi Range and Traffic Control for Defence Networks. *Defence Science Journal*, *75*, 100–110. https://doi.org/10.14429/dsj.75.20284

Khan, A. U., Khan, M. E., Hasan, M., Zakri, W., Alhazmi, W., & Islam, T. (2022). An Efficient Wireless Sensor Network Based on the ESP-MESH Protocol for Indoor and Outdoor Air Quality Monitoring. In *Sustainability* (Vol. 14, Issue 24, p. 16630). https://doi.org/10.3390/su142416630

Li, X., & Si, W. E. I. (2025). Research on Deep Learning-Based Optimization Algorithms for IoT Communication. *IEEE Access*, *13*(June), 177724–177744. https://doi.org/10.1109/ACCESS.2025.3597098

Macaia, A., Narayan, N., Shukla, R., Chandra, A., Zelený, O., Zavorka, R., Blumenstein, J., Prokes, A., Wojtun, J.,

E-ISSN :2962-1658
Volume 5, Number 2, April 2026
https://doi.org/10.47709/ijmdsa.v5i2.8076

Kelner, J., & Ziółkowski, C. (2025). *Framework for Indoor Wireless Propagation Modeling Through Wireless Insite®*. https://doi.org/10.1109/RADIOELEKTRONIKA65656.2025.11008377

Manual, T. R. (n.d.). *Technical Reference Manual*.

Mendoza, R., Monton, J., & Dellosa, J. (2024). *IoT-Based Energy Monitoring System for Optimizing Power Consumption in University Facilities*. https://doi.org/10.1109/IDAP64064.2024.10710764

Orie, R., Otabil, L., Agorua, J., & Iqbal, M. T. (2025). Enhanced IoT-Based Optimization for a Hybrid Power System in Cartwright, Labrador. In *Energies* (Vol. 18, Issue 7, p. 1566). https://doi.org/10.3390/en18071566

Plauska, I., Liutkevičius, A., & Janavičiūtė, A. (2023). Performance Evaluation of C/C++, MicroPython, Rust and TinyGo Programming Languages on ESP32 Microcontroller. In *Electronics* (Vol. 12, Issue 1, p. 143). https://doi.org/10.3390/electronics12010143

Rahimifar, A., & Kavian, Y. S. (2025). A Review on Energy Efficiency in Software-Defined Wireless Sensor Networks for IoT Applications. *2025 Fifth National and the First International Conference on Applied Research in Electrical Engineering (AREE)*, 1–6. https://doi.org/10.1109/AREE63378.2025.10880302

Ravilla, L., Upadhyay, S., Louis, M. T., Swain, B., & Mamatha, G. N. (2025). *Energy-Efficient Protocols for Massive IOT Connectivity in 6G Networks*. *5*(1), 550–553.

Sabo, A., Suleiman, H., Dahiru, Y., Jatau, N., Yusuf, A., & Chikodi, A. (2024). Development and Implementation of an ESP32 IOT-Based Smart Grid for Enhanced Energy Efficiency and Management. *European Journal of Theoretical and Applied Sciences*, *2*, 565–576. https://doi.org/10.59324/ejtas.2024.2(3).43

Singh, R., Berkvens, R., & Weyn, M. (2020). *Energy Efficient Wireless Communication for IoT Enabled Greenhouses*. https://doi.org/10.1109/COMSNETS48256.2020.9027392

Sridevi, & Kolhar, A. (2025). *Energy-Efficiency Strategies for Wireless Sensor Networks in IoT* (pp. 167–192). https://doi.org/10.4018/979-8-3373-0300-0.ch006

Systems, E. (2025a). *ESP32 Wi-Fi Driver*. Espressif Systems. https://docs.espressif.com/projects/esp-idf/en/v5.0/esp32/api-guides/wifi.html

Systems, E. (2025b). *ESP32 Wi-Fi Driver Overview*. Espressif Systems. https://docs.espressif.com/projects/esp-idf/en/latest/esp32/api-guides/wifi-driver/overview.html

Tradacete-Ágreda, M., Sánchez-Pérez, A., Santos-Pérez, C., Hueros-Barrios, P. J., Rodríguez-Sánchez, F. J., & Espolio-Maestro, J. (2025). Smart Energy Management for Residential PV Microgrids: ESP32-Based Indirect Control of Commercial Inverters for Enhanced Flexibility. In *Sensors* (Vol. 25, Issue 21, p. 6595). https://doi.org/10.3390/s25216595

Urazayev, D., Eduard, A., Ahsan, M., & Zorbas, D. (2023). *Indoor Performance Evaluation of ESP-NOW*. https://doi.org/10.1109/SIST58284.2023.10223585